Monthly Notices
of the
ROYAL ASTRONOMICAL SOCIETY

MNRAS **445,** 1205–1212 (2014) doi:10.1093/mnras/stu1831

Hard X-ray emission of Sco X-1

Mikhail G. Revnivtsev,[1⋆] Sergey S. Tsygankov,[1,2,3] Eugene M. Churazov[1,4] and Roman A. Krivonos[1,5]

[1]*Space Research Institute, Russian Academy of Sciences, Profsoyuznaya 84/32, 117997 Moscow, Russia*
[2]*Finnish Centre for Astronomy with ESO (FINCA), University of Turku, Väisäläntie 20, FI-21500 Piikkiö, Finland*
[3]*Tuorla Observatory, Department of Physics and Astronomy, University of Turku, Väisäläntie 20, FI-21500 Piikkiö, Finland*
[4]*Max-Planck-Institute für Astrophysik, Karl-Schwarzschild-Str. 1, D-85740 Garching bei München, Germany*
[5]*Space Sciences Laboratory, University of California, Berkeley, CA 94720, USA*

Accepted 2014 September 4. Received 2014 August 15; in original form 2014 April 18

ABSTRACT

We study hard X-ray emission of the brightest accreting neutron star Sco X-1 with *INTEGRAL* observatory. Up to now *INTEGRAL* have collected ∼4 Ms of deadtime corrected exposure on this source. We show that hard X-ray tail in time average spectrum of Sco X-1 has a power-law shape without cutoff up to energies ∼200–300 keV. An absence of the high energy cutoff does not agree with the predictions of a model, in which the tail is formed as a result of Comptonization of soft seed photons on bulk motion of matter near the compact object. The amplitude of the tail varies with time with factor more than 10 with the faintest tail at the top of the so-called flaring branch of its colour–colour diagram. We show that the minimal amplitude of the power-law tail is recorded when the component, corresponding to the innermost part of optically thick accretion disc, disappears from the emission spectrum. Therefore, we show that the presence of the hard X-ray tail may be related with the existence of the inner part of the optically thick disc. We estimate cooling time for these energetic electrons and show that they cannot be thermal. We propose that the hard X-ray tail emission originates as a Compton upscattering of soft seed photons on electrons, which might have initial non-thermal distribution.

Key words: stars: individual: Sco X-1 – X-rays: binaries.

1 INTRODUCTION

Sco X-1 is the brightest X-ray source on the sky. Its emission in X-ray energy band is powered by energy released in accretion of matter on to neutron star (NS) in a semidetached binary system. Sco X-1 receives a lot of attention because while studying such a bright source one can try to test theoretical models of the accretion flow with maximally possible precision.

The vast majority of X-ray emission of Sco X-1 (as well as of other NS binaries with high mass accretion rates) is formed in two parts of the accretion flow – in optically thick accretion disc (see model of Shakura & Sunyaev 1973) and optically thick layer between the accretion disc and the NS surface (e.g. Mitsuda et al. 1984). Both these regions have temperatures about few keV and emit thermal spectra in 1–20 keV energy band.

In addition to these components, already early observations of Sco X-1 showed that sometimes an additional power-law-like component is present at energies above 20–40 keV (Peterson & Jacobson 1966; Agrawal et al. 1971; Haymes et al. 1972; Duldig et al. 1983), but sometimes not (Lewin, Clark & Smith 1967; Coe et al. 1980; Rothschild et al. 1980; Maisack et al. 1994). More recent studies of NS binaries at high mass accretion rates confirmed that amplitude of a hard X-ray power-law component varies with time and likely correlates with detailed characteristics of spectral state of the source (D'Amico et al. 2001; Di Salvo et al. 2001, 2002, 2006; Paizis et al. 2006; D'Aí et al. 2007; Sturner & Shrader 2008; Maiolino, D'Amico & Braga 2013).

The origin of this tail remains unclear. Among different models of formation of this tail one can mention synchrotron emission of energetic electrons (e.g. Riegler 1970), Comptonizaion of seed photons on electrons of hot thermal corona, on non-thermal electrons (e.g. Di Salvo et al. 2006), or on bulk motion of matter near the compact object (e.g. Paizis et al. 2006; Farinelli et al. 2009). In order to distinguish between these models, one need to obtain high-quality spectral energy distribution in hard X-rays because of possible high energy cutoff, predicted by some models, and to relate the behaviour of the hard X-ray tail to other components of X-ray emission of the source. In this paper, we will try to do this with the help of data of *INTEGRAL* orbital observatory.

At present the best instrument to study the hard X-ray/soft gamma-ray emission of Sco X-1 is *INTEGRAL* observatory

⋆ E-mail: revnivtsev@iki.rssi.ru

(Winkler et al. 2003). This observatory has the best ever available sensitivity to hard X-ray emission, especially at energies above 150–200 keV. During more than 10 years of operation this observatory performed more than 2000 separate observing sessions with combined exposure time (before dead time correction) about 5.7 Ms (including 4 Ms of observations, granted to authors of this paper). Sensitivity of the combined data set reaches the level ∼1 mCrab at energies ∼150 keV and ∼5 mCrab at energies 200–300 keV.

2 DATA ANALYSIS AND THE SAMPLE

We used all publicly available data of *INTEGRAL* observatory (Winkler et al. 2003) on Sco X-1, including those, granted to authors of this paper (4 Ms of proposal ID 0720011). In total the data set contains 2032 individual pointings.

Two main instruments of *INTEGRAL* observatory: IBIS (Ubertini et al. 2003; Lebrun et al. 2003) and SPI (Vedrenne et al. 2003) cover a broad energy range from ∼20 keV to ∼10 MeV. We used data of instruments IBIS/ISGRI and SPI, which provide the best sensitivities at energies 20–500 keV. X-ray monitor JEM-X of *INTEGRAL* observatory has field of view ∼4.°8 much smaller than those of IBIS and SPI (∼9° and ∼16° correspondingly), and therefore have collected much less exposure on Sco X-1 (observations of *INTEGRAL* is composed of a set of individual pointings – dithering pattern – which span 10°in both directions). Therefore, in order to extend our energy coverage down to 3 keV used simultaneous observations with *RXTE* observatory.

2.1 IBIS/ISGRI data analysis

Total exposure of IBIS/ISGRI observations is ∼5.7 Ms before deadtime correction and ∼3.8 Ms after deadtime correction.

INTEGRAL/IBIS/ISGRI data were processed with the method described in Revnivtsev et al. (2004) and Krivonos et al. (2007, 2010). The spectral characteristics of the ISGRI detector changes with time, which leads to variations of the spectral gain (conversion of instrumental channels to photon energies) and energy resolution of the instrument (see e.g. Caballero et al. 2013). In order to put data of all ISGRI observations into proper energy scale, we have performed gain corrections for all individual observations with the help of fluorescence line of tungsten at ∼59 keV characteristic of the ISGRI background (Terrier et al. 2003; Tsygankov et al. 2006; Caballero et al. 2013). Therefore, at energies around 60 keV we can estimate an uncertainty of channel-to-energy conversion to be less than ∼0.5 keV, while at lower energies 20–30 keV this uncertainty can increase up to 1–2 keV, or ∼1 per cent. Thus, in all our subsequent analysis we assume that the accuracy of our values, related with the energy scale is not better than ∼1 per cent.

For all observations we have produced a set of images in a number of energy intervals. The raw count rate of sources determined from these images was corrected for two main effects: offset-angle-dependent absorption of X-rays in IBIS mask support structure and long-term variations of the instrument characteristics. These effects were measured with the help of numerous observations of Crab nebula, which we consider to be a stable source. Correction for absorption in the IBIS mask support structure was done with the help of simple axisymmetric analytic function, fitted to the Crab nebula observations, performed at different offsets. Time-dependent count rate correction was done using Crab nebula count rates, averaged over 400 d time bins.

The resulting light curves of the Crab nebula, corrected for these two main effects, nevertheless still have residual variances exceeding those caused by a Poisson statistics. In energy band 17–26 keV, the residual rms variations have amplitude 5.7 per cent, in energy band 26–38 keV 4.2 per cent, in energy band 38–57 keV 4.2 per cent and in energy band 57–86 keV 4.5 per cent. At higher energies, the rms variations of the corrected count rates, measured in individual pointings (∼1–2 ks exposure time) are already compatible or less than those created by Poisson statistics. In our study, we treat the remaining residuals as being artificial due to various unaccounted instrumental effects, while existence of small (at the level of a few per cent) intrinsic variations of the Crab nebula hard X-ray flux is still possible (see e.g. study of Crab nebula flux variations in Wilson-Hodge et al. 2011). The limited accuracy of the inferred Crab nebula flux stability means that our sensitivity to Sco X-1 spectral variations is limited by these systematic uncertainties, which we should keep in mind in the subsequent analysis. All model fits to *INTEGRAL* data points take into account these additional systematic uncertainties at the level of 4–5 per cent.

2.2 SPI data analysis

In addition to the ISGRI data, we utilized data obtained with the SPI spectrometer on board *INTEGRAL* observatory. It operates in energy range from 20 keV to 8 MeV and complements the IBIS telescope in studies of hard emission from compact objects. Coded aperture mask gives to the spectrometer imaging capabilities with an angular resolution of 2.°5 (FWHM).

Primary data screening and reduction was done following procedures described in Churazov et al. (2005, 2011).

The model used to derive the spectrum consists of a single point source (at the position of Sco X-1) and a constant (two free parameters for each energy channel). For individual observations, the response to a point source is calculated using Instrument Response Functions (IRFs). This model is then applied to the background subtracted SPI data and the best-fitting fluxes from the source in narrow energy channels form the Sco X-1 spectrum.

To reduce an undesirable contribution from the Galactic diffuse emission and other point sources located in the Galactic Centre region, we selected only observations, in which the centre of the SPI field of view was within 10° circle around Sco X-1. The total net exposure time of used SPI observations is about 4.3 Ms.

Inclusion to the sky model additional point sources in the SPI field of view (1E 1740.7−294, GX 1+4, 4U 1700−377, MAXI J1659−152) and Galactic diffuse emission does not affect significantly the resultant spectrum of Sco X-1.

2.3 *RXTE*/PCA data analysis

In order to extend the energy spectrum of the source down to 3 keV, we have studied spectra of Sco X-1, obtained by spectrometer PCA of *RXTE* observatory Bradt, Rothschild & Swank (1993) during time periods of *INTEGRAL* observations (similar to those in works of Di Salvo et al. 2006; Sturner & Shrader 2008). All data were analysed with standard tasks of HEASOFT v6.15.

3 TWO PATTERNS OF FLUX VARIATIONS

The spectrum of Sco X-1, averaged over all analysed observations is presented in Fig. 1. Spectra measured by two *INTEGRAL* instruments are perfectly consistent with each other.

Long-term light curve of Sco X-1 is shown in Fig. 2 (the source fluxes here and below are shown in units of Crab nebula count rate in appropriate energy ranges). It is seen that the hard X-ray flux of

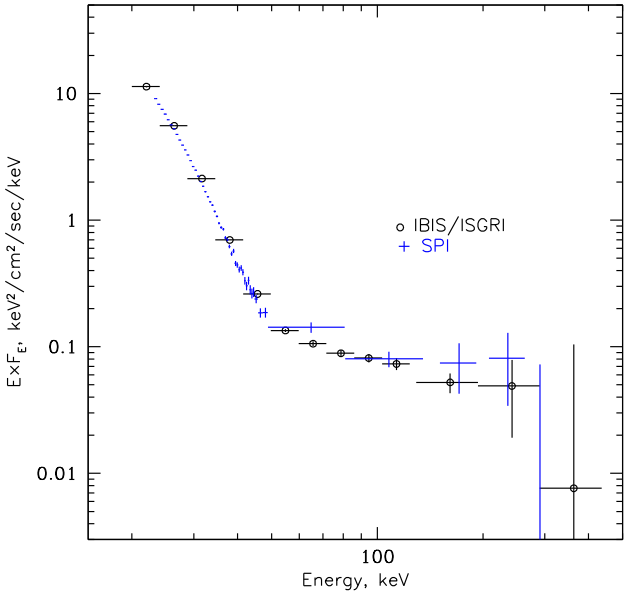

Figure 1. Spectrum of Sco X-1 in hard X-rays measured by *INTEGRAL* instruments, averaged over all observations. Open circles denote spectrum, measured by IBIS/ISGRI instrument, crosses with SPI.

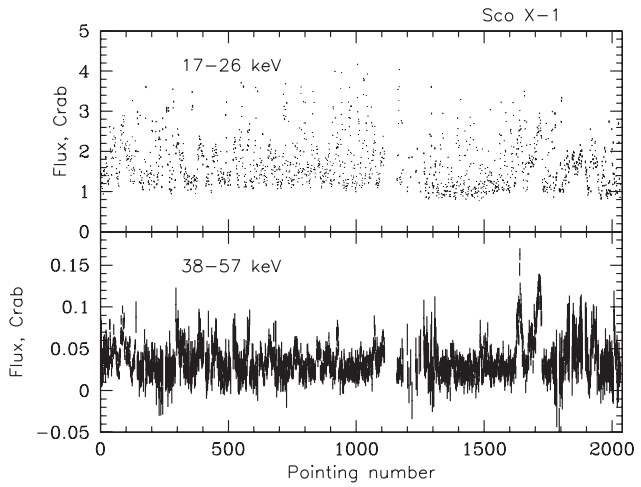

Figure 2. Light curve of Sco X-1 as measured by IBIS/ISGRI in units of Crab nebula count rate in the same energy ranges. X-axis here shows the running number of *INTEGRAL* pointings. We present the light curve in such a way because of big gaps between different sections of observations.

Sco X-1 is strongly variable, at the level far exceeding instrumental uncertainties (see description of systematic in Section 2.1).

Time variability of Sco X-1 fluxes has two branches. We can see that strong variability of the source flux in 17–26 keV energy range can be either accompanied by similar variability at harder X-rays (38–57 keV) or not. The spectacular example of such bimodality can be seen at data points closer to the end of our data set. The close-up to this set of points is shown in Fig. 3.

Spectra, illustrating the two branches are shown in Fig. 5.

The spectrum collected in observations, occupying the lower-right corner of the flux–flux diagram (region A in Fig. 4), has virtually no power-law tail and can be adequately fitted with simple thermal component. The best-fitting analytical approximation can be done by an exponential cutoff $\mathrm{d}N/\mathrm{d}E \propto E^0 \exp(-E/E_{\rm cut})$ with $E_{\rm cut} = 3.70 \pm 0.03$ keV or blackbody emission with $kT = 2.8 \pm 0.05$ keV.

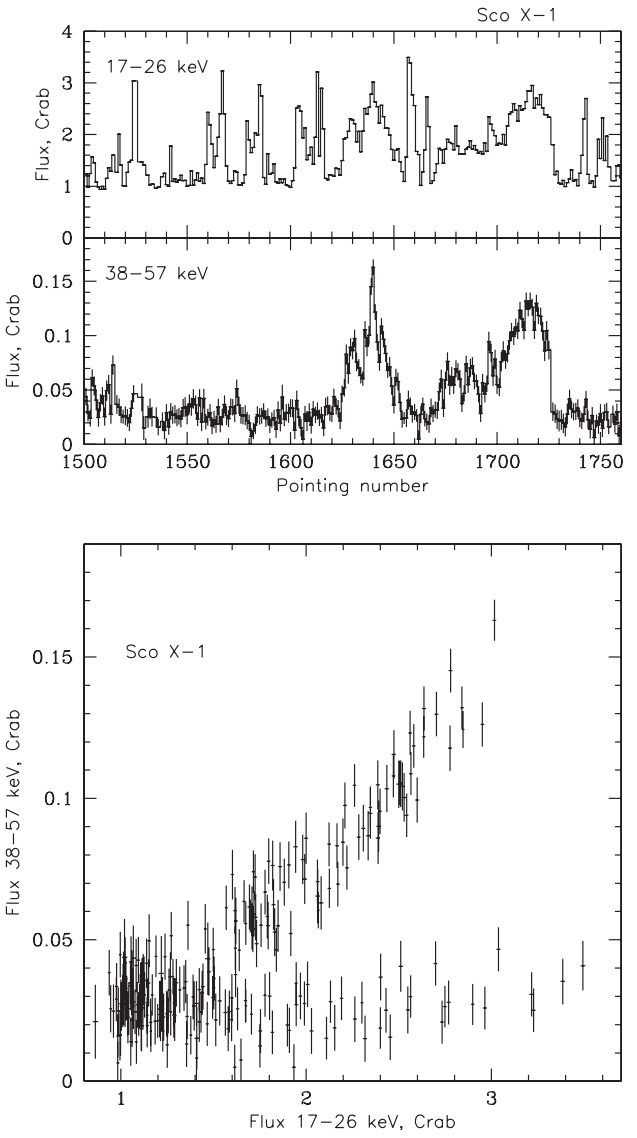

Figure 3. Upper panel: light curve of Sco X-1 in energy bands 17–26 keV and 38–57 keV during some part of observations, selected around hard X-ray flares. Lower panel: flux–flux diagram of these light curves.

The upper-right part of the diagram is formed by spectra, with significant power-law tail. Spectrum collected within this region (region B) is shown by open triangles in Fig. 5. The hard X-ray part of this spectrum (above 60 keV) can be described by a power law with photon index $\Gamma = 2.6 \pm 0.3$ without high energy cutoff. The exact value of the lower limit on the cutoff energy depends on assumed functional shape of the model. For simple exponential cutoff, the lower limit (2σ) is $E_{\rm cut} > 330$ keV. The 50–250 keV flux in this tail is $\sim$4–5 $\times$ 10^{-10} erg cm^{-2} s^{-1}.

4 RELATION OF THE TAIL WITH OTHER SPECTRAL COMPONENTS

It was previously shown (Di Salvo et al. 2001, 2006; D'Aí et al. 2007) that the presence of the tail in spectra of bright NS binaries is

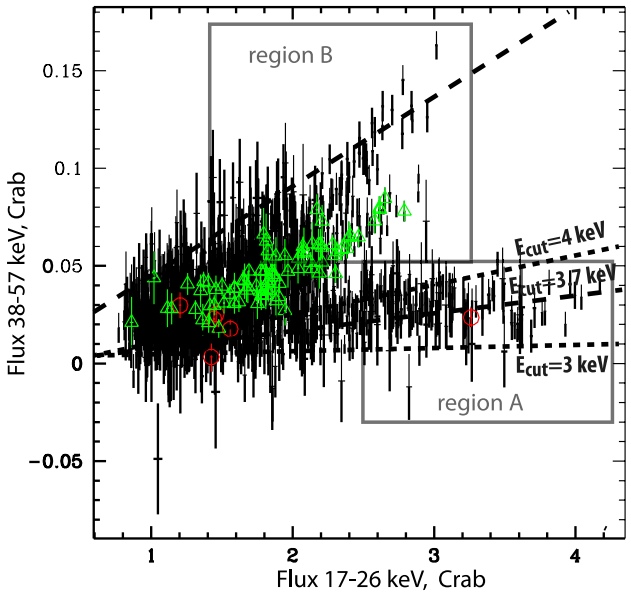

Figure 4. Flux–flux diagram of light curves of Sco X-1 in energy bands 17–26 keV and 38–57 keV, presented for all observational data set. Open triangles and circles show fluxes of Sco X-1, measured during observations, performed simultaneously with *RXTE*. Open triangles denote observations in horizontal and normal branches, open circles denote those on flaring branch. Dashed line shows correlation of two fluxes, which corresponds to spectral shape $dN/dE \propto \exp(-E/E_{cut})$ with $E_{cut} = 3.7$ keV, appropriate for emission of the boundary/spreading layer on NS surface. Upper and lower dotted lines show correlation $E_{cut} = 4$ and 3 keV, respectively.

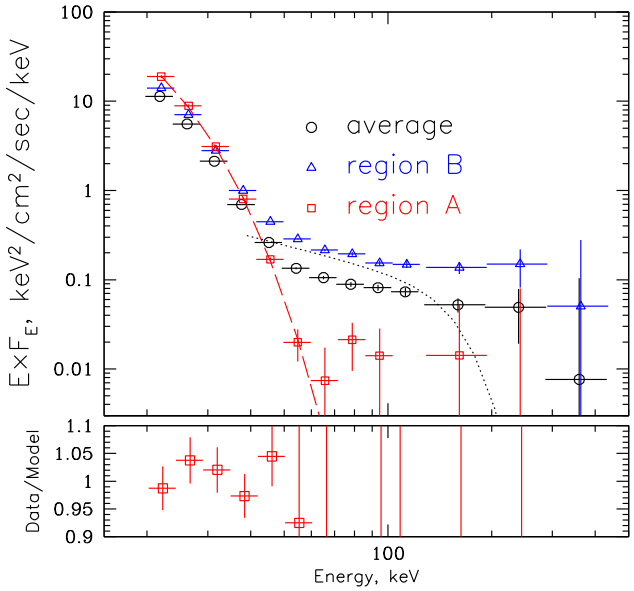

Figure 5. Spectra of Sco X-1, collected during different time periods. Open circles denote time-averaged source spectrum, open triangles spectrum collected within sector A of Fig. 4, open squares spectrum collected within sector B of Fig. 4. Dashed curve shows simple analytic model $dN/dE \propto \exp(-E/3.7\,\mathrm{keV})$, representing emission of the boundary/spreading layer on NS surface. Dotted curve – simple analytical fit (following receipt of Zdziarski et al. 2001) to Monte Carlo simulation of emission Comptonized by bulk motion of matter around black holes (Laurent & Titarchuk 1999). Bottom panel shows data to model ratio of maximally tail-free spectrum of Sco X-1 (red open squares). It is seen that up to statistically significant points at 60 keV the data to model ratio is within our adopted systematic uncertainties of ∼4–5 per cent.

related with position of sources on colour–colour diagram (CCD). The maximally luminous tail is observed on the so-called horizontal and normal branches of CCD (see e.g. Hasinger & van der Klis 1989, for description of CCD phenomenology) and the weakest power-law tail – on the flaring branch.

While physical origin of different branches on CCD of bright NS binaries is not yet understood in details, several important clues are already obtained.

Spectral decomposition of emission of luminous NS binaries is a complicated issue due to similarity of spectral shapes of two main components: optically thick accretion disc and a boundary/spreading layer (see e.g. different decompositions in Di Salvo et al. 2002; D'Aí et al. 2007). In our work, we adhere approach of model-independent decomposition, based on properties of variability of luminous NS, outlined in works of Gilfanov, Revnivtsev & Molkov (2003) and Revnivtsev & Gilfanov (2006).

In these works, it was shown that energy spectra of bright NS binaries (at least in energy band 1–20 keV) may be decomposed into contribution of optically thick accretion disc with temperatures $kT \sim 1$–1.8 keV and the NS surface with colour temperature $kT \sim 2.5$–2.7 keV. The latter has virtually constant spectral shape over the whole range of luminosities and spectral hardnesses unless the source transit into optically thin regime of emission (Mitsuda et al. 1984; Gilfanov et al. 2003; Revnivtsev & Gilfanov 2006).

Stability of the hotter thermal component spectral shape can be understood as Eddington limited emission of optically thick radiation pressure dominated spreading/boundary layer, where matter settles from rapid rotation in accretion disc to slower rotation of the NS (Inogamov & Sunyaev 1999; Suleimanov & Poutanen 2006).

Variations of hardness (colours) of observed X-ray emission of bright NS binaries in energy band 2–20 keV occur due to variations of the accretion disc temperature and its fractional contribution to the total X-ray emission.

It was shown that at the top part of the flaring branch the X-ray emission of bright NS binaries consists of almost solely the NS surface/boundary/spreading layer (Revnivtsev, Suleimanov & Poutanen 2013). Contribution of the innermost parts of optically thick accretion disc drops significantly to almost undetectable levels while the total source brightness might increase in this state. Origin of such a decrease of the accretion disc component contribution is not clear yet and requires further study.

We should emphasize again here that this conclusion is based on spectral decomposition, which uses information about the source flux variability. The decompositions based on spectral modelling only may provide different results (see e.g. D'Aí et al. 2007).

As an illustration of such behaviour of Sco X-1 we present Fig. 6. As the accretion disc contribution in energy spectrum is visible only at energies below 10 keV we cannot limit ourselves with data of IBIS and SPI instruments of *INTEGRAL* observatory (operating at energies >20 keV). In order to reach energies about 3 keV and to maximize the statistics we used data of simultaneous observations of Sco X-1 with IBIS/*INTEGRAL* and PCA/*RXTE*. Requirement of simultaneity of *INTEGRAL* and *RXTE* observations leaves only a small fraction of all available data sets.

In Fig. 6, we present broad-band spectra collected at the top and the bottom parts of the 'flaring branch' (128 s exposure time of *RXTE*/PCA at energies 3–20 keV). Both spectra were fitted as a sum of boundary/spreading layer component (we adopted simple analytic form $dN/dE \propto E^0 \exp(-E/3.7\,\mathrm{keV})$ following Gilfanov

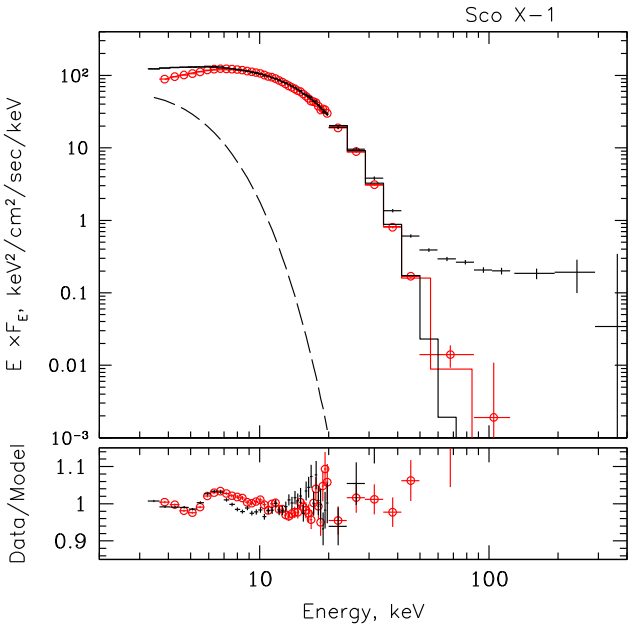

Figure 6. X-ray spectra of Sco X-1 at two spectral states. Red crosses show spectrum collected on flaring branch of its CCD evolution, *INTEGRAL*/IBIS data collected over region A in Fig. 4, at softer X-rays we use *RXTE*/PCA data at the top of the flaring branch (128 s spectrum). Black crosses show spectrum at horizontal branch of Sco X-1, *INTEGRAL*/IBIS data collected over region B of Fig. 4, at softer X-ray we use *RXTE*/PCA data (128 s) within time interval shown by topmost triangle on Fig. 4. Spectra are scaled vertically to match at energies 15–25 keV. Solid red (grey) histogram shows analytic model of boundary/spreading layer on NS surface (see text), long-dashed curve shows multicolour blackbody disc component. It is seen that disappearance of the power-law tail in spectrum is accompanied by disappearance of multicolour disc component. Bottom panel shows the ratio of the data points to the simple model, consisting of contribution of the accretion disc and the boundary/spreading layer. The iron fluorescent emission line at ∼6.4 keV, not included in the model, is clearly seen in the residuals.

et al. 2003; Revnivtsev & Gilfanov 2006; Revnivtsev et al. 2013) and multicolour disc blackbody component (Shakura & Sunyaev 1973; Mitsuda et al. 1984). We see that while at the bottom of the flaring branch the multicolour disc contribution is comparable (or even larger) than that of the boundary/spreading layer, on top of the flaring branch this contribution is absent.

Therefore, the difference of the top part of the flaring branch from any other branches of Sco X-1 is the absence of the spectral component attributed to the innermost optically thick accretion disc. Note, that similar (in terms of spectral component analysis) disruption of the inner disc was previously observed in black hole candidates GRS 1915+105 (Belloni et al. 1997).

Study of hard X-ray emission of Sco X-1 shows that the power-law hard X-ray tail also disappears at this stage. In Fig. 4, flaring branch observations are denoted by open circle.

From this plot, we can make two important conclusions.

(i) Contribution of hard X-ray power-law tail is small at the top part of the flaring branch (similar conclusion was previously obtained by Di Salvo et al. 2006 and Sturner & Shrader 2008).

(ii) Variations of fluxes in energy bands 17–26 keV and 38–57 keV on the top of the flaring branch (i.e. without power-law tail) occur with constant spectral shape (the straight line best fit to the data points within region A on flux–flux diagram of Fig. 4 has a reduced χ^2/d.o.f. ∼1.18, while within region B it has a value χ^2/d.o.f. ∼ 3.06). This conclusion strongly supports our previous findings (Gilfanov et al. 2003; Revnivtsev & Gilfanov 2006; Revnivtsev et al. 2013) that the hotter thermal component, which we ascribe to emission of the boundary/spreading layer on NS surface, preserve its shape over all flux variation of bright NS binaries. These hard X-ray observations are important because at these energies $E > 10kT$ our sensitivity to variations of the colour temperature of the thermal component is exponentially high (at energies $E \gg kT$ even small variations of the colour temperature of the emission lead to large variations of the spectral hardness).

Making use of our variability-based spectral decomposition (Gilfanov, Revnivtsev & Molkov 2003; Revnivtsev & Gilfanov 2006) and basing on above-mentioned arguments, we conclude that the hard X-ray power-law tail in spectrum of Sco X-1 may be related with existence of the innermost part of the optically thick accretion disc and not with hotter thermal component (boundary/spreading layer emission). This might reflect difference in energy release mechanisms in magneto-rotational instability-dominated accretion disc and in the slowly decelerating spreading layer on NS surface (Inogamov & Sunyaev 1999, 2010). It is expected that in the former case powerful corona should form (see e.g. Miller & Stone 2000; Schnittman, Krolik & Noble 2013), while it might not form in the latter case.

5 PHYSICAL ORIGIN OF THE TAIL

The vast majority of X-ray emission of Sco X-1 is generated in optically thick accretion disc and boundary/spreading layer. Hard X-ray tail, which does not have an exponential cutoff up to at least 200–300 keV, should be generated within some optically thin region with energetic electrons and the tail should not be directly associated with the emission of NS surface (the tail is not seen during time periods with exclusive contribution of the NS surface/boundary/spreading layer). In this case, it is reasonable to seek for analogies with the emission mechanisms of accreting stellar mass black holes.

Studies of emission of accreting black holes showed that optically thin regions with energetic electrons exist in two flavours (see e.g. review in Done, Gierliński & Kubota 2007). First – as optically thin part of the accretion flow inside some distance from the compact object, where the optically thick disc is truncated, the hot electrons in this region are thermalized and the emitting spectrum can be described by Comptonization on thermal electrons (Shapiro, Lightman & Eardley 1976; Sunyaev & Truemper 1979; Poutanen, Krolik & Ryde 1997). Secondly – as region, where hard X-ray/soft gamma-ray tail in energy spectra of bright accreting black hole systems does not show evidences of thermal cutoff. The widely accepted interpretation of this emission is a Compton upscattering of some seed photons on hybrid/non-thermal electrons (see e.g. Coppi 1999; Gierliński et al. 1999; Zdziarski et al. 2001).

Among other mechanisms, which were proposed for generation of hard X-ray/soft-gamma-ray tail in emission spectra of accretion discs, one can mention Comptonization on bulk motion of electrons, moving with relativistic speed close to the black hole horizon (Mastichiadis & Kylafis 1992; Titarchuk, Mastichiadis & Kylafis 1997; Laurent & Titarchuk 1999). In some studies, similar mechanism was also considered for accreting NS (see e.g. Paizis et al. 2006; Farinelli et al. 2009).

The capability of this mechanism to produce the observed hard X-ray tails in spectra of accreting black holes was discussed in details in Zdziarski et al. (2001). It was shown that the main con-

tradiction of bulk motion Comptonization models with the data is inevitable rollover of their predicted energy spectra in hard X-rays. The cutoff energy in the spectrum depends on the bulk radial velocity of the matter close to the compact object and cannot be higher than $E_{\rm cut} \sim m_{\rm e}c^2/{\rm few} \sim 100$–$200$ keV (see e.g. Laurent & Titarchuk 1999; Zdziarski et al. 2001; Farinelli et al. 2012). The most sensitive observations of some black hole binaries show a power-law tail without noticeable cutoff up to energies 500–600 keV.

In the case of Sco X-1, we have statistically significant spectral data points up to ∼200 keV. In order to visualize the spectral shape of the bulk Comptonization model (for the extreme case of accreting black hole from work of Laurent & Titarchuk 1999), we present dotted curve on Fig. 5. This curve represents analytic approximation (from Zdziarski et al. 2001) of Monte Carlo simulated bulk motion Comptonization spectrum. It is clear that even in this case of assumed accretion on to black hole, in which the bulk motion velocities of matter are significantly higher than those in the case of accreting NS, the spectrum has a cutoff at ∼150 keV and this cutoff strongly contradicts the observed spectral data points.

For pure free-fall on to NS with radius $R_{\rm NS} = 3R_{\rm g}$, the maximum radial velocity of the matter corresponds to $\beta = v_{\rm r}/c < 0.6$, which is already smaller than that near black holes. In the case of accreting NS with emerging luminosities close to the Eddington limit (e.g. Sco X-1), the bulk radial velocity of the matter should be even smaller than that. This should result in even smaller cutoff energy in the spectrum of the tail (see e.g. numerical models in Farinelli et al. 2012).

Therefore, we can conclude that obtained hard X-ray spectrum of Sco X-1 does not agree with the predictions of a model, in which the hard X-ray tail is formed as a result of Comptonization of some seed photons on bulk motion of the matter around accreting compact object.

Thermal Comptonization of seed photons in hot (with temperatures above 100 keV, which might create an observed power-law tail up to energies >200–300 keV) optically thin inner part of the accretion flow does not seem to be probable because huge soft photon flux from NS surface ($L_{\rm soft} > 10^{38}$ erg s^{-1}) with Compton temperature around few keV very effectively cools down (via Compton cooling) any possible hot ($\gtrsim$100 keV) thermal flow.

Compton cooling time for energetic electron can be estimated as

$$t_{\rm Compt} \lesssim \pi \gamma^{-1} l_{\rm s}^{-1} \frac{R}{c},$$

where $l_{\rm s}$ is the soft emission compactness:

$$l_{\rm s} = \frac{L_{\rm soft}}{R} \frac{\sigma_T}{m_{\rm e}c^3} > 600.$$

Here, we adopted that the size the emitting region R does not exceed few NS radii (because we assume that it is related with the innermost parts of the accretion flow), i.e. $R \lesssim 5 \times 10^6$ cm. We see that the Compton cooling time for electrons is significantly less than the light crossing time of the emitting region.

Thermalization time for electrons in this region depends on processes, which determine the energy exchange. Coulomb scattering of relativistic electrons of energies $\gamma m_{\rm e}c^2$ with thermal bath of non-relativistic electrons thermalize them on time-scale (see e.g. Stepney 1983; Svensson 1999)

$$t_{\rm Coulomb} \sim \frac{\gamma^2}{\tau_{\rm Th} \ln \Lambda} \left(\frac{R}{c}\right)$$

that is larger than $t_{\rm Compt}$ in our case of relativistic electrons in optically thin $\tau_{\rm Th} < 1$ region. Here, ln Λ is the Coulomb logarithm and $\tau_{\rm Th}$ the Thomson optical depth of the region. Exchange of energies between electrons due to synchrotron self-absorption (the so-called synchrotron boiler mechanism; Ghisellini, Guilbert & Svensson 1988; Svensson 1999; Malzac & Belmont 2009) in a region with magnetic compactness $l_{\rm B}$:

$$l_{\rm B} = \frac{\sigma_{\rm T}}{m_{\rm e}c^2} R \frac{B^2}{8\pi},$$

gives thermalization time:

$$t_{\rm synch} \sim \gamma^{-1} l_{\rm B}^{-1} \frac{R}{c},$$

which in our case ($l_{\rm s} \gg l_{\rm B}$) is larger than Compton cooling timescale.

We can conclude that in the absence of some special collisionless plasma mechanisms of thermalization the optically thin hot plasma in the innermost accretion flow cannot be uniformly thermal because the electrons do not have time to thermalize. The hard X-ray photons emerging in the tail (above 50–60 keV) should be result of Compton upscattering of soft photons on electrons having their original distribution. This original distribution can be non-thermal (see e.g. simulation of reconnection events; Zenitani & Hoshino 2001; Yamada, Kulsrud & Ji 2010), depending on the physical mechanism of energy input into electron population.

We can assume that one of the most probable scenario of generation of hard X-ray tail in spectrum of Sco X-1 is a non-thermal Comptonization in some corona-like regions above the accretion disc (see e.g. scenario of Galeev, Rosner & Vaiana 1979). Such scenario have direct analogy with accreting black holes in the so-called soft state. According to the widely accepted model, during this state the accretion to a black hole occurs via optically thick disc with optically thin corona above it. Optically thick disc emits blackbody-like emission, while optically thin corona with energetic electrons upscatters these soft photons to higher energies (see e.g. Coppi 1999; Gierliński et al. 1999; Done et al. 2007). This optically thick disc should be very similar to that around NS in Sco X-1; therefore, we can anticipate that somewhat similar corona-like flow above this disc can also exist in this case.

An example of the spectrum, expected in such hybrid thermal/non-thermal plasma (model *eqpair* of Coppi 1999 in XSPEC package; Arnaud 1996) is presented in Fig. 7.

For this energy spectrum we assumed that the hybrid/non-thermal plasma upscatters only photons from accretion disc and adopted the following parameters: $l_{\rm nth} = 0.99$ fraction of energy deposited into non-thermal electrons with the power-law slope $\Gamma = 3$, soft photons luminosity compactness $l_{\rm s} = 600$, fraction of the energy, inserted into hard component with respect to the soft component $l_{\rm h}/l_{\rm s} =$ 0.6 per cent, temperature of the soft (blackbody) photons emission $kT_{\rm bb} = 1.1$ keV.

We should note here that energetic electrons in this optically thin corona can upscatter not only photons from optically thick accretion disc, but also photons from the NS surface (boundary/spreading layer). This should result in modest changes of the shape of the spectral model, shown in Fig. 7, but more quantitative description of this modification will depend on not known geometry of the Comptonizing region and is beyond the scope of this paper.

6 SUMMARY

We have studied all available data of *INTEGRAL* observatory on hard X-ray emission of the brightest accreting NS Sco X-1. In total,

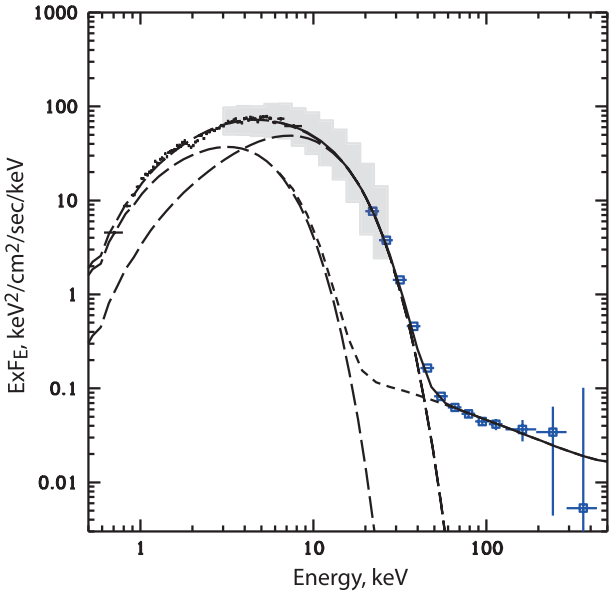

Figure 7. Broad-band energy spectrum of Sco X-1. At energies below 7 keV crosses show data points, measured with ASCA observatory (observation 1993 Aug. 16), at energies 3–20 keV grey stripe denotes the rms-range of spectral densities, measured by *RXTE*/PCA over around 700 observations, collected during the period 1996–2012. At energies above 20 keV, open squares show time-averaged spectrum of Sco X-1, measured with *INTEGRAL*/IBIS/ISGRI. Long-dashed curves denote contribution of an accretion disc (left curve) and a boundary/spreading layer (right curve) components. Short-dashed curve shows the prediction of a model, in which soft blackbody photons with $kT = 1.1$ keV are Comptonized by hybrid/non-thermal plasma (model *eqpair*, see the text for other parameters). Solid line is a sum of all components.

it sum up to ∼6 Ms of astronomical time and ∼4 Ms of deadtime corrected exposure time. Our results can be summarized as follows.

(i) Time-averaged spectrum of Sco X-1 contains hard X-ray tail which has a power-law shape without cutoff up to energies ∼200–300 keV.

(ii) This allows us to conclude that obtained hard X-ray spectrum of Sco X-1 does not agree with the predictions of a model, in which the hard X-ray tail is formed as a result of Comptonization of some seed photons on bulk motion of the matter around accreting compact object.

(iii) The amplitude of the tail varies with time with factor more than 10.

(iv) We confirm previous findings that amplitude of the hard X-ray tail in energy spectrum of Sco X-1 correlates with its position on CCD. The faintest tail is seen at the top of the so-called flaring branch.

(v) Our spectral decomposition of the energy spectrum of Sco X-1 shows an absence (or significant decrease of contribution) of optically thick accretion disc component at the top part of the flaring branch. Therefore, we conclude that the presence of the hard X-ray tail may be related with the existence of the inner part of the optically thick disc.

(vi) Assuming that hard X-ray tail is generated above the innermost part of optically thick accretion disc, we estimate cooling time for energetic electrons and show that they cannot be uniformly thermal. We conclude that the hard X-ray tail emission originates as a Compton upscattering of soft seed photons on electrons, which have intrinsically non-thermal distribution.

ACKNOWLEDGEMENTS

Research is based on observations with *INTEGRAL*, an ESA project with instruments and science data centre funded by ESA member states (especially the PI countries: Denmark, France, Germany, Italy, Switzerland, Spain), Czech Republic and Poland, and with the participation of Russia and the USA. Research has made use of data obtained through the High Energy Astrophysics Science Archive Research Center Online Service, provided by the NASA/Goddard Space Flight Center. Authors thank Max Planck Institute fuer Astrophysik for computational support. The work was supported by Russian Scientific Foundation (RNF), project 14-22-00271.

REFERENCES

Agrawal P. C., Biswas S., Gokhale G. S., Iyengar V. S., Kunte P. K., Manchanda R. K., Sreekantan B. V., 1971, Ap&SS, 10, 500
Arnaud K. A., 1996, in Jacoby G. H., Barnes J., eds, ASP Conf. Ser. Vol. 101, Astronomical Data Analysis Software and Systems V. Astron. Soc. Pac., San Francisco, p. 17
Belloni T., Mendez M., King A. R., van der Klis M., van Paradijs J., 1997, ApJ, 479, L145
Bradt H. V., Rothschild R. E., Swank J. H., 1993, A&AS, 97, 355
Caballero I. et al., 2013, in Goldwurm A., Lebrun F., Winkler C., eds, Proc. 9th Int. Workshop, INTEGRAL IBIS/ISGRI energy calibration in OSA 10. Paris, France, p. 6
Churazov E., Sunyaev R., Sazonov S., Revnivtsev M., Varshalovich D., 2005, MNRAS, 357, 1377
Churazov E., Sazonov S., Tsygankov S., Sunyaev R., Varshalovich D., 2011, MNRAS, 411, 1727
Coe M. J. et al., 1980, ApJ, 237, 148
Coppi P. S., 1999, in Poutanen J., Svensson R., eds, ASP Conf. Ser. Vol. 161, High Energy Processes in Accreting Black Holes. Astron. Soc. Pac., San Francisco, p. 375
D'Aí A., Życki P., Di Salvo T., Iaria R., Lavagetto G., Robba N. R., 2007, ApJ, 667, 411
D'Amico F., Heindl W. A., Rothschild R. E., Gruber D. E., 2001, ApJ, 547, L147
Di Salvo T., Robba N. R., Iaria R., Stella L., Burderi L., Israel G. L., 2001, ApJ, 554, 49
Di Salvo T. et al., 2002, A&A, 386, 535
Di Salvo T. et al., 2006, ApJ, 649, L91
Done C., Gierliński M., Kubota A., 2007, A&AR, 15, 1
Duldig M. L., Greenhill J. G., Fenton K. B., Thomas R. M., Watts D. J., 1983, Ap&SS, 95, 137
Farinelli R., Paizis A., Landi R., Titarchuk L., 2009, A&A, 498, 509
Farinelli R., Ceccobello C., Romano P., Titarchuk L., 2012, A&A, 538, A67
Galeev A. A., Rosner R., Vaiana G. S., 1979, ApJ, 229, 318
Ghisellini G., Guilbert P. W., Svensson R., 1988, ApJ, 334, L5
Gierliński M., Zdziarski A. A., Poutanen J., Coppi P. S., Ebisawa K., Johnson W. N., 1999, MNRAS, 309, 496
Gilfanov M., Revnivtsev M., Molkov S., 2003, A&A, 410, 217
Hasinger G., van der Klis M., 1989, A&A, 225, 79
Haymes R. C., Harnden F. R., Jr, Johnson W. N., III, Prichard H. M., Bosch H. E., 1972, ApJ, 172, L47
Inogamov N. A., Sunyaev R. A., 1999, Astron. Lett., 25, 269
Inogamov N. A., Sunyaev R. A., 2010, Astron. Lett., 36, 848
Krivonos R., Revnivtsev M., Lutovinov A., Sazonov S., Churazov E., Sunyaev R., 2007, A&A, 475, 775
Krivonos R., Revnivtsev M., Tsygankov S., Sazonov S., Vikhlinin A., Pavlinsky M., Churazov E., Sunyaev R., 2010, A&A, 519, A107
Laurent P., Titarchuk L., 1999, ApJ, 511, 289
Lebrun F. et al., 2003, A&A, 411, L141
Lewin W. H. G., Clark G. W., Smith W. B., 1967, ApJ, 150, L153
Maiolino T., D'Amico F., Braga J., 2013, A&A, 551, L2
Maisack M., Kendziorra E., Pan H., Skinner G., Englhauser J., Reppin C., Efremov V., Sunyaev R., 1994, ApJS, 92, 473

Malzac J., Belmont R., 2009, MNRAS, 392, 570
Mastichiadis A., Kylafis N. D., 1992, ApJ, 384, 136
Miller K. A., Stone J. M., 2000, ApJ, 534, 398
Mitsuda K. et al., 1984, PASJ, 36, 741
Paizis A. et al., 2006, A&A, 459, 187
Peterson L. E., Jacobson A. S., 1966, ApJ, 145, 962
Poutanen J., Krolik J. H., Ryde F., 1997, MNRAS, 292, L21
Revnivtsev M. G., Gilfanov M. R., 2006, A&A, 453, 253
Revnivtsev M. G. et al., 2004, Astron. Lett., 30, 382
Revnivtsev M. G., Suleimanov V. F., Poutanen J., 2013, MNRAS, 434, 2355
Riegler G. R., 1970, Nature, 226, 1041
Rothschild R. E. et al., 1980, Nature, 286, 786
Schnittman J. D., Krolik J. H., Noble S. C., 2013, ApJ, 769, 156
Shakura N. I., Sunyaev R. A., 1973, A&A, 24, 337
Shapiro S. L., Lightman A. P., Eardley D. M., 1976, ApJ, 204, 187
Stepney S., 1983, MNRAS, 202, 467
Sturner S. J., Shrader C. R., 2008, Proc. 7th INTEGRAL Workshop (PoS(Integral08)041), The Hard X-Ray Emission from Scorpius X-1 as Seen by INTEGRAL. p. 41, available at: http://pos.sissa.it/cgi-bin/reader/conf.cgi?confid=67)
Suleimanov V., Poutanen J., 2006, MNRAS, 369, 2036
Sunyaev R. A., Truemper J., 1979, Nature, 279, 506
Svensson R., 1999, in Poutanen J., Svensson R., eds, ASP Conf. Ser. Vol. 161, High Energy Processes in Accreting Black Holes. Astron. Soc. Pac., San Francisco, p. 361
Terrier R. et al., 2003, A&A, 411, L167
Titarchuk L., Mastichiadis A., Kylafis N. D., 1997, ApJ, 487, 834
Tsygankov S. S., Lutovinov A. A., Churazov E. M., Sunyaev R. A., 2006, MNRAS, 371, 19
Ubertini P. et al., 2003, A&A, 411, L131
Vedrenne G. et al., 2003, A&A, 411, L63
Wilson-Hodge C. A. et al., 2011, ApJ, 727, L40
Winkler C. et al., 2003, A&A, 411, L1
Yamada M., Kulsrud R., Ji H., 2010, Rev. Mod. Phys., 82, 603
Zdziarski A. A., Grove J. E., Poutanen J., Rao A. R., Vadawale S. V., 2001, ApJ, 554, L45
Zenitani S., Hoshino M., 2001, ApJ, 562, L63

This paper has been typeset from a TEX/LATEX file prepared by the author.